1-3-2005

Integration of epitaxial colossal magnetoresistive films onto Si(100) using $SrTiO_3$ as a template layer

Aswini K. Pradhan
Center for Materials Research, Norfolk State University, apradhan@nsu.edu

S. Mohanty
Center for Materials Research, Norfolk State University, Norfolk, Virginia

Kai Zhang
Center for Materials Research, Norfolk State University, Norfolk, Virginia

J.B. Dadson
Center for Materials Research, Norfolk State University, Norfolk, Virginia

E.M. Jackson
Center for Materials Research, Norfolk State University, Norfolk, Virginia

See next page for additional authors

Integration of epitaxial colossal magnetoresistive films onto Si(100) using $SrTiO_3$ as a template layer

A. K. Pradhan,[a] S. Mohanty, Kai Zhang, J. B. Dadson, E. M. Jackson, D. Hunter, R. R. Rakhimov, and G. B. Loutts
Center for Materials Research, Norfolk State University, 700 Park Avenue, Norfolk, Virginia 23504

Jun Zhang and D. J. Sellmyer
Department of Physics and Astronomy and Center for Materials Research and Analysis, University of Nebraska, Lincoln, Nebraska 68588-0113

(Received 15 July 2004; accepted 29 October 2004; published online 23 December 2004)

We report on the integration of epitaxial colossal magnetoresistive $La_{0.67}Ba_{0.33}MnO$ films on Si(100) semiconductor using $SrTiO_3$ template layer by pulsed-laser deposition. X-ray diffraction reveals the superior quality of the manganite film that grows epitaxially on heteroepitaxially grown $SrTiO_3$ template layer on Si substrate. The epitaxial films demonstrate remarkable surface morphology, magnetic transition and hysteresis, magnetoresistance, and ferromagnetic resonance, illustrating the ferromagnetic nature of the film and possible device applications at room temperature. © *2005 American Institute of Physics*. [DOI: 10.1063/1.1842852]

There has been a considerable research interest recently to integrate perovskite-type oxide thin films onto Si, not only to meet the ever-shrinking size of the metal-oxide-semiconductor field-effect transistors (FETs) for application as alternative high-k gate dielectrics, devices such as dynamic random access memories, ferroelectric nonvolatile memories, but also a template layer to integrate other perovskites, such as lanthanum-based colossal magnetoresistive (CMR) oxides onto Si for application in FETs for spintronic, high-density magnetic memory, sensors, and infrared bolometers[1–8] at ambient temperature. Among all reported high-k materials, perovskite-type $SrTiO_3$ (STO) lends itself one of the most potential materials for an alternative gate dielectric if high-quality epitaxial STO films are grown on Si. STO has a simple cubic structure with $k=300$ at room temperature and the lattice mismatch between STO ($a_0=3.905$ Å) and Si ($a_0=5.431$ Å) is reasonably small ($\sim 1.7\%$) with STO unit cell rotated 45° around Si surface normal to [001] axis. STO films of very high structural quality are deposited by molecular-beam epitaxy[8] and the availability of such high-quality [001] perovskite-terminated Si[100] substrates provides numerous opportunities for integration of other technologically important perovskites, such as CMR, on a surface of high crystalline quality.

While perovskite lanthanum-based manganite ($R_{1-x}B_xMnO_3$ where R and B are rare-earth and alkali metals, respectively) films have been successfully grown on single-crystal oxide substrates, such as STO, $LaAlO_3$, and $NdGaO_3$, the growth on Si is very limited.[8] It is also of a great importance to integrate an IR detector array with complementary metal-oxide-semiconductor readout as well as FET architecture on the same Si wafer. However, the results achieved on Si are very limited. In order to grow an epitaxial quality manganite film, the film–substrate lattice mismatch needs to be minimized, the film–substrate thermal expansion coefficients have to be matched, and the chemical reaction between the substrate and deposited film should be eliminated. Although Si does not comply with all these requirements, introducing a template layer can accommodate mechanical and chemical disaccords. Furthermore, the biaxial strain due to lattice mismatch between film and substrate that plays a dominant role for the electronic phase separation and it modifies the charged ordered state in CMR materials.[7,8] This lattice strain induced by the substrate in epitaxial films of these materials can be used as a good parameter for tuning the physical properties through the mutual coupling of the lattice degree of freedom to the charge, spin, and orbital degrees of freedom.[9–12] However, integrating the manganites onto the semiconducting materials such as Si, GaAs, and GaN remains a challenging task for potential device applications that utilize both information processing and data storage in the same device. Recent progress on direct integration[8,13] of STO on Si has opened a possibility to integrate both STO and $R_{1-x}B_xMnO_3$ onto this technologically important semiconductor. In this letter, we report fabrication of superior-quality $La_{0.67}Ba_{0.33}MnO$ [(LBMO)/STO/Si(001)] heterostructures, using pulsed-laser deposition (PLD), which demonstrate remarkable structural, microscopic, and magnetic properties in the vicinity of room temperature. We have demonstrated highly epitaxial growth of LBMO on Si using a heteroepitaxially grown STO template layer.

LBMO/STO/Si(100) epitaxial films were grown by a multitarget PLD technique (KrF excimer, $\lambda=248$ nm) with a pulse energy density of $1-2$ J/cm^2 and utilizing both target rotation and rastering, and substrate rotation facilities. Single crystalline STO and high-density LBMO targets were used. LBMO calcined powders were isostatically pressed at 400 MPa and sintered at 1450 °C in order to make a high-density target. The films were deposited on clean Si (100) substrates with a substrate temperature 700–800 °C, keeping oxygen partial pressure of 200 to 400 mTorr. The substrate was loaded to the chamber using load-lock facility attached to the chamber, and heated in the chamber just after the ultimate base pressure $<4\times10^{-8}$ Torr to avoid the oxidation of the substrate. For STO/Si growth, the initial 2-nm-thick growth of STO film was carried out without using oxygen gas, and subsequently 18-nm-thick film of STO

[a]Author to whom all correspondence should be addressed; electronic mail: apradhan@nsu.edu

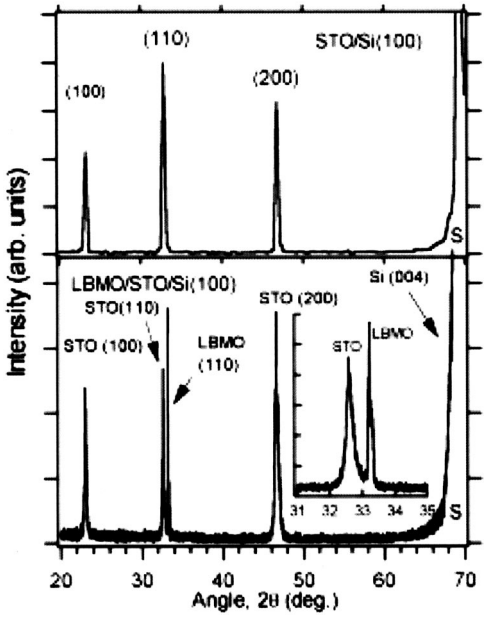

FIG. 1. XRD patterns of STO/Si(100) (top) and LBMO/STO/Si (bottom) heterostructures. The inset (bottom) shows the rocking curve XRD pattern of LBMO/STO/Si heterostructures, showing growth of LBMO on STO template layer gown on Si.

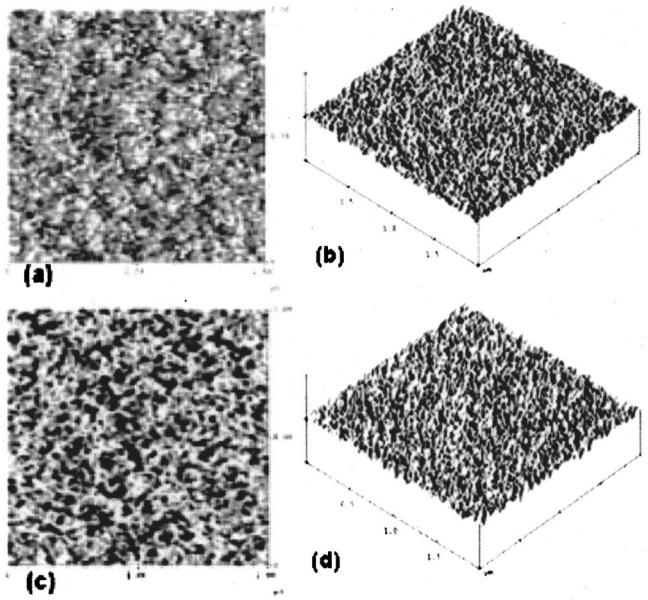

FIG. 2. AFM images of (a) and (b) STO/Si, and (c) and (d) LBMO/STO/Si heterostructures. All images are 2 μm$\times$2 μm in size.

on Si was deposited with oxygen partial pressure of 1 mTorr with laser repetition rate of 3 Hz. Several batches of STO/Si films were grown in order to optimize the best condition to obtain good-quality epitaxial film. LBMO film of 50 nm was immediately deposited in oxygen partial pressure on STO/Si using a laser repetition rate of 5 Hz. The film was cooled in 1 Torr of oxygen partial pressure to room temperature. The x-ray diffraction (XRD) of the films was done in a Rigaku x-ray diffractometer using Cu K_α radiation. The zero-field-cooled magnetization (M) and hysteresis measurements were carried out down to 5 K using a superconducting quantum interference device magnetometer (Quantum Design), and the resistivity measurements were done with a four-probe technique. The ferromagnetic resonance (FMR) experiments were done in a Bruker EMS spectrometer operating at 9.6 GHz microwave frequency.

Figure 1 shows the XRD patterns of STO/Si and LBMO/STO/Si films. The XRD of the STO/Si heterostructure reveals strong (l00) orientations. However, a strong STO(110) orientation was also observed. The orientation relationship between the STO thin film and the Si(001) substrate in the STO/Si heterostructure is described[13,14] as $(001)_{STO}//(001)_{Si}$ and $(100)_{STO}//(110)_{Si}$, which means the STO lattice is rotated by 45° around the [001] axis of the Si lattice on the Si(001) surface. The lattice misfit parameter between Si(110) (3.82 Å) and STO (3.905 Å) is about 1.67%, which is reasonably small[14] between the parallel interfaces and could induce very small strain. The observation of a strong STO(110) orientation is favored for the growth of STO/Si heterostructure due to similar lattice matching. A strong satellite reflection of $(011)_{STO}$ was seen in the selected area electron diffraction pattern[14] taken from an interface region, illustrating the orientation relationship of $(100)_{STO}//(110)_{Si}$. In LBMO/STO/Si heterostructures, LBMO preferred energetically to grow epitaxially only in (110) orientation on $(110)_{STO}$ direction due to reduced strain as shown in the bottom of Fig. 1. The rocking curve of epitaxial growth of LBMO on $(110)_{STO}$ is shown in the inset of Fig. 1. The full widths at half-maximum of STO(110) and LBMO(110) are about 0.3° and 0.1°, respectively, which illustrate the highly crystalline nature of the film.

In order to compare the surface morphology of STO/Si and LBMO/STO/Si films, atomic force microscopic (AFM) images are shown in Figs. 2(a)–2(d). The atomically flat and defect-free surface morphology with rms surface roughness of less than 2 nm was seen in STO/Si film. Surprisingly, closer inspection of the AFM images of STO/Si reveals heteroepitaxial growth on the surface. However, LBMO/STO/Si film shows very uniform and epitaxial surface morphology with similar surface roughness and crystallite size $<$20 nm. These studies suggest good crystallinity and epitaxy in all films.

In Fig. 3(a), the zero-field-cooled temperature dependence of magnetization is shown for LBMO/STO/Si film in a field of 0.1 T. The magnetic transitions are fairly sharp with T_c onset at 320 K, as shown in the top inset of Fig. 3(a). The films demonstrate ferromagnetic hysteresis at 300 K with a ferromagnetic saturation field of about 4 KOe, as shown in the inset of Fig. 3. The temperature and magnetic field dependence of resistivity ρ show a remarkably sharp jump at the metal–insulator transition temperature (T_{MI}) as shown in Fig. 3(b), which is consistent with the magnetic transition. The T_{MI} is remarkably sharp, and the calculated value of temperature coefficient of resistivity [TCR$=1/\rho$ dρ/dT $\approx$20% at T_{MI}, as shown in the inset of Fig. 3(b)] is very much relevant for the required value for the bolometric applications. The resistivity is significantly reduced at the transition with the magnetic field due to spin alignment. However, the onset of T_c is slightly higher compared to the films grown directly on STO substrates.[6,15] The T_c value for $x=0.33$ film is about 305 K compared to that of its bulk, with $T_c=345$ K. The difference in T_c in films compared to their bulk counterpart is certainly attributed to the type of strain developed between the films and the substrates. The role of the strain-induced modification of the $d_{x^2-y^2}$ orbital stability resulting from in-plane Mn-O distance determines the T_c of

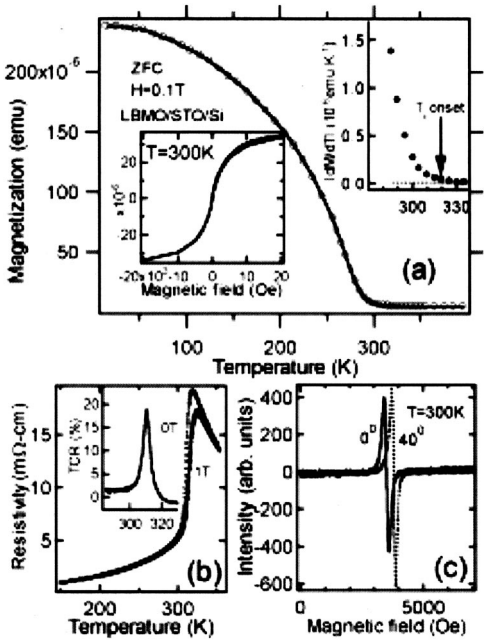

FIG. 3. (a) Temperature-dependent zero-field-cooled magnetization of LBMO/STO/Si film for a magnetic field of 0.1 T. The top inset shows dM/dT vs temperature. The bottom inset shows magnetization hysteresis loops of film at room temperature, illustrating ferromagnetic behavior. (b) The temperature dependence of resistivity of LBMO/STO/Si film in 0 T and 1 T magnetic fields. The inset in (b) shows the TCR(%) as function of temperature. (c) Ferromagnetic resonance spectra of LBMO/STO/Si film at room temperature for two angles.

LBMO[6,12] through Mn^{3+}-O-Mn^{4+} double-exchange mechanism. As a consequence, the effective in-plane charge density decreases in case of compressive strain. It has been shown[12] that the lattice mismatch induces compressive-type strain for $x=0.33$ ($c/a\approx 0.15\%$), which is responsible for reducing T_c in LBMO films, contrary to other CMR material. However, the superior nano-crystallinity, epitaxial nature of LBMO/STO/Si film, and especially the epitaxial STO template layer can minimize the strain effect through strain relaxation for enhanced transition. There remain enough scopes to minimize the interface disorders and to enhance the oxygenation to markedly enhance the physical properties in the vicinity of room temperature.

It is also remarkable to note that the heterostructures display a pronounced ferromagnetic resonance at room temperature [Fig. 3(c)]. The spectra present a characteristic feature centered at about $g=2$. However, the resonant field position changes with angle between the film surface and the applied magnetic field, indicating the anisotropic behavior of the epitaxial film. Although the effective demagnetization field, $4\pi M_{\text{eff}}=4\pi M_s-2K_u/M_s$ (where M_s is saturation magnetization and K_u is anisotropy energy density perpendicular to the film plane) is different, the variation could arise from different residual stress in the film. The present FMR signal is mainly from the Mn^{4+} ions, which is close to $g=1.994$, since the contribution from Mn^{3+} ions is unlikely to produce an observable signal due to their large zero-field splitting and strong spin-lattice relaxation.[16]

It is anticipated that further optimization of the growth process may enhance the magnetic properties of the heterostructure significantly. Our studies are significantly different from other reports[7,8] wherein manganites films are grown on Si using several buffer layers. However, the present LBMO/STO/Si heterostructures are unique in the sense that both manganites and STO could lead to multifunctionalities for various technological applications.

In summary, we have demonstrated the fabrication and high performance of epitaxial manganite films grown on Si substrates using $SrTiO_3$ as a template layer with a T_c tuned to room temperature. The epitaxial films demonstrate remarkable surface morphology, magnetic hysteresis, magnetic transition, and ferromagnetic resonance at room temperature, illustrating the ferromagnetic nature of the film. Our results demonstrate the scope of the integration of epitaxial manganite films on semiconducting substrates, such as Si, and can be extended to other potential semiconductors, such as GaN and GaAs, using appropriate template/buffer layers. This will produce many generic approaches to the integration of multicomponent oxide thin films on semiconducting surfaces, which can impact a variety of technologies.

This work is supported by the National Aeronautics and Space Administration and University Research Center cooperative agreement NCC-3-1035 and National Science Foundation for Center for Research Excellence in Science and Technology grant no. HRD-9805059. One of the authors (R.R.R.) acknowledges the support from the faculty research program provided by NASA. Research at the University of Nebraska is supported by NSF-MRSEC, ONR, and CMRA. Authors are thankful to A. Wilkerson for experimental help.

[1] A. Goyal, M. Rajeswari, R. Shreekala, S. E. Lofland, S. M. Bhagat, T. Boettcher, C. Kwon, R. Ramesh, and T. Venkatesan, Appl. Phys. Lett. **71**, 2535 (1997).
[2] M. Rajeswari, C. H. Chen, A. Goyal, C. Kwon, M. C. Robson, R. Ramesh, T. Venkatesan, and S. Lakeou, Appl. Phys. Lett. **68**, 3555 (1996).
[3] S. Mathews, R. Ramesh, T. Venkatesan, and J. Benedetto, Science **276**, 3790 (1997).
[4] M. Rajeswari, R. Shreekala, A. Goyal, S. E. Lofland, S. M. Bhagat, K. Ghosh, R. P. Shaema, R. L. Greene, R. Ramesh, and T. Venkatesan, Appl. Phys. Lett. **73**, 2672 (1998).
[5] R. von Helmolt, J. Wecker, B. Holzapfel, L. Schultz, and K. Samwer, Phys. Rev. Lett. **71**, 2331 (1993); S. Jin, T. H. Tiefel, M. McCormack, R. A. Fastnacht, and R. Ramesh, Science **264**, 413 (1994).
[6] A. K. Pradhan, D. Sahu, B. K. Roul, and Y. Feng, Appl. Phys. Lett. **81**, 3597 (2002).
[7] T. Zhao, S. B. Ogale, S. R. Shinde, R. Ramesh, R. Droopad, J. Yu, K. Eisenbeiser, and J. Misewich, Appl. Phys. Lett. **84**, 750 (2004).
[8] J.-H. Kim, S. I. Khartsev, and M. Grishin, Appl. Phys. Lett. **82**, 4295 (2003), and references therein.
[9] Y. Suzuki, H. Y. Hwang, S.-W. Cheong, and R. B. van Dover, Appl. Phys. Lett. **71**, 140 (1997); F. Tsui, M. C. Smoak, T. K. Nath, and C. B. Eom, *ibid.* **76**, 2421 (2000).
[10] Y. Ogimoto, M. Izumi, T. Manako, T. Kimura, Y. Tomioka, M. Kawasaki, and Y. Tokura, Appl. Phys. Lett. **78**, 3505 (2001).
[11] E. R. Buzin, W. Prellier, Ch. Simon, S. Mercone, B. Mercey, B. Raveau, J. Sebek, and J. Hejtmanek, Appl. Phys. Lett. **79**, 647 (2001).
[12] J. Zhang, H. Tanaka, T. Kanki, J.-H. Choi, and T. Kawai, Phys. Rev. B **64**, 184404 (2001).
[13] Y. Wang, C. Ganpule, B. T. Liu, H. Li, K. Mori, B. Hill, M. Wuttig, R. Ramesh, J. Finder, Z. Yu, R. Droopad, and K. Eisenbeiser, Appl. Phys. Lett. **80**, 97 (2002), and references therein.
[14] G. Y. Yang, J. M. Finder, J. Wang, Z. L. Wang, Z. Yu, J. Ramdani, R. Droopad, K. W. Eisenbeiser, and R. Ramesh, J. Mater. Res. **17**, 204 (2002).
[15] A. K. Pradhan, D. Sahu, B. K. Roul, and Y. Feng, J. Appl. Phys. **96**, 1170 (2004).
[16] A. Shengelaya, G. M. Zhao, H. Keller, and F. A. Muller, Phys. Rev. Lett. **77**, 5296 (1996).